

Analysis of compression-induced chiral phase separation in Langmuir monolayers

Wei Zhao, Chen-Xu Wu, and Mitsumasa Iwamoto

Department of Physical Electronics, Tokyo Institute of Technology, 2-12-1 O-Okayama, Meguro-ku, Tokyo 152-8552, Japan

(Received 24 August 1999; revised manuscript received 12 November 1999)

We analyze the compression-induced chiral phase separation (CPS) in Langmuir films, taking into account the elastic theory of liquid crystals and the mixing energy of the two constituent enantiomers. The difference between the Selinger-Wang-Bruinsma-Knobler theory [J. V. Selinger *et al.*, Phys. Rev. Lett. **70**, 1139 (1993)] and our treatment is that we do not introduce the concentration-square-gradient term in the free energy, but alternatively take into account a line tension at CPS boundaries. Our model predicts that a two-domain pattern with opposite chiralities is energy minimized, but a multistripe pattern with two alternate constant chiralities is also possible, though metastable. This offers a tentative explanation for the CPS pattern consisting of homogeneously oriented stripes with diverse widths observed by Eckhardt *et al.* [Nature (London) **362**, 614 (1993)].

PACS number(s): 61.30.Cz, 64.70.Md, 68.10.-m, 68.15.+e

I. INTRODUCTION

As interesting topics, chiral symmetry breaking (CSB), chiral discrimination, and chiral phase separation (CPS) have been extensively investigated [1–5]. It is believed that in two-dimensional (2D) systems the issue should be simplified [6]. Experimentally, a large number of observations of pattern formation on 2D systems, such as freely suspended films of smectic liquid crystals [7–9], Langmuir monolayers [9–13], and Langmuir-Blodgett (LB) films [14], are believed to be associated with CSB. Among these experiments, the contribution of Eckhardt *et al.* [12] is quite noticeable. They studied the Langmuir monolayers of a kind of chiral tetracyclic alcohol and observed three phases at different surface pressures. At high pressure, using atomic force microscopy (AFM), they imaged the formation of parallel stripes with alternate molecular packings, as well as large areas of uniform domains with mirror-symmetric positional orders. The racemic composition of the monolayer, as well as the existence of mirror-symmetric positional orders, strongly implies the occurrence of CPS.

Selinger *et al.* made a valuable attempt to build a universal description of CSB in 2D systems [the Selinger-Wang-Bruinsma-Knobler (SWBK) theory] [15]. In this penetrating work, SWBK invoked a Ginzburg-Landau-type free energy containing the Frank elastic energy in terms of the 2D tilt director field $\hat{\mathbf{c}}(\mathbf{r})$,

$$F_s = \int d^2r \left[\frac{1}{2} \kappa (\nabla \psi)^2 + \frac{1}{2} t \psi^2 + \frac{1}{4} u \psi^4 + \frac{1}{2} K_1 (\nabla \cdot \hat{\mathbf{c}})^2 + \frac{1}{2} K_3 (\nabla \times \hat{\mathbf{c}})^2 - \lambda \psi \nabla \times \hat{\mathbf{c}} \right]. \quad (1)$$

Here ψ is the chiral order parameter and $\hat{\mathbf{c}} = (\cos \phi, \sin \phi)$ is the normalized tilt director field. The first three terms in F are the standard Ginzburg-Landau expansion in powers of ψ . The coefficient t refers to temperature. The next two terms are the Frank energy of the director field. The last term is the coupling between the chiral order parameter and the director field. SWBK established a phase diagram in terms of temperature t and coupling coefficient λ , which includes four

phases: a uniform nonchiral one, a striped one, a square lattice one, and a uniform chiral one. The striped phase is sinusoidal at high temperature and solitonlike at low temperature.

SWBK pointed out three kinds of CSB mechanisms in 2D systems: (i) a hexatic phase with tilt direction between the nearest and next-nearest directions, (ii) a nonhexatic phase with inequivalent molecular packings on the surface that are mirror images of each other, or (iii) a phase formed of chiral domains, each containing just one type of enantiomer. It is the third case that relates to the CPS of enantiomers.

The striped patterns predicted by SWBK are fairly similar to the observed conformations. However, there are substantial inconsistencies between the predicted textures and the observed patterns in Langmuir monolayers and LB films [9,16]. This may be reflected in three aspects. (i) In both the sinusoidal and the solitonlike striped patterns predicted, the azimuthal angle ϕ varies with position; however, the observations on Langmuir monolayers and LB films revealed the uniformity of molecular packing in each domain (see Figs. 3 and 4 in Ref. [12], Fig. 3 in Ref. 13, and Fig. 1 in Ref. [14]). (ii) The SWBK theory may not easily explain the diversity of the stripe widths, i.e., why the stripes in Fig. 4 in Ref. [12] are several nanometers wide, whereas in c and d of Fig. 3 in the same work, there is no stripe texture in the $10 \times 10 \text{ nm}^2$ area; moreover, the stripes shown in Fig. 4 of that work also have diverse widths. (iii) Several observations implied that the domain boundaries are walls with abrupt changes of composition and molecular packing [7–9,12]. For example, the sharp mutations of molecular packing at boundaries shown in Ref. [12] are evident, with only one or two lines of intermediate molecules. This is not readily consistent with the predictions of SWBK. Ohyama *et al.* [17] improved the SWBK theory by permitting the variation of the length of the 2D director field, whereas these inconsistencies still remain.

It is worth mentioning that Seul and Andelman [18] reviewed two approaches to depict the spatial variation of concentration in Langmuir monolayers in one of their articles about phase transition and pattern formation. One is based on the Ginzburg-Landau expansion, used by Andelman *et al.* [19] and many other researchers in similar topics. The other is the direct employment of a line tension γ at domain walls

instead, which is also widely used [20]. The only difference between these two approaches is that the former includes a concentration-square-gradient (CSG) term $(\nabla\psi)^2$ in its free energy, whereas the latter has a line energy γL at boundaries instead. Here L is the length of the boundary. As indicated by Seul and Andelman, these two approaches are equivalent in a sense. Cahn and Hilliard gave an elegant analysis of this equivalence in their classic paper on the surface tension between two phases of a binary alloy [21], for which we give a parallel demonstration for the 2D racemic mixture in the Appendix.

Now let us return to the current topic. The SWBK theory is actually relevant to the first approach mentioned above. In a previous work [22], we built a description of compression-induced CPS in Langmuir monolayers, viewing a monolayer as a film of cholesteric liquid crystal [23] and taking into account the mixing energy of the two enantiomers by a Bragg-Williams approximation [24]. In this paper, we clarify that in fact this model is associated with the second approach. In Ref. [20], the line tension at phase boundary is introduced basically as an assumption, while in our model it is a natural consequence of the chiral discrimination between enantiomers. On the basis of this model, we give here a tentative interpretation for the aforementioned inconsistencies between the SWBK theory and the experimental results. Briefly, this model depicts the CPS boundary as a wall accompanied by a line tension, and predicts patterns consisting of uniform stripes with homogeneous chirality and molecular packing in each stripe. This picture is in accordance with the experimental results.

In Sec. II, we will compare the free energy of the present model with that of the SWBK theory. The mathematical treatment and the prediction of possible patterns will be demonstrated in Sec. III. Section IV will be devoted to discussing the compression-induced CPS. Finally, we will conclude this work in Sec. V.

II. FREE ENERGY

In the present model, the free energy of a monolayer consisting of two enantiomers is written as [22]

$$\begin{aligned}
 F = & \int \frac{1}{2} l \cos \theta [k_{11}(\nabla \cdot \mathbf{d})^2 + k_{22}(\mathbf{d} \cdot \nabla \times \mathbf{d})^2 \\
 & + k_{33}(\mathbf{d} \times \nabla \times \mathbf{d})^2 - 2k_2(\mathbf{d} \cdot \nabla \times \mathbf{d})] dA + \frac{k_B T}{A_0} \\
 & \times \int [\chi \ln \chi + (1-\chi) \ln(1-\chi) + \alpha_0 \chi(1-\chi)] dA \\
 & + \lambda_L \int (\chi - \frac{1}{2}) dA.
 \end{aligned} \tag{2}$$

Here the first integral is the Frank elastic energy of cholesteric liquid crystals, with $\mathbf{d} = (\sin \theta \cos \phi, \sin \theta \sin \phi, \cos \theta)$ being the three-dimensional (3D) director. k_{11} , k_{22} , and k_{33} are the elastic constants, and k_2 is the chiral modulus. The second integral is the mixing energy of the two enantiomers in Bragg-Williams form. $\chi = N_D(\mathbf{r})/[N_L(\mathbf{r}) + N_R(\mathbf{r})]$ is the local chiral order parameter. A_0 is the average molecular area and l is the molecular length. $\alpha_0 = 4w/k_B T$ is the chiral dis-

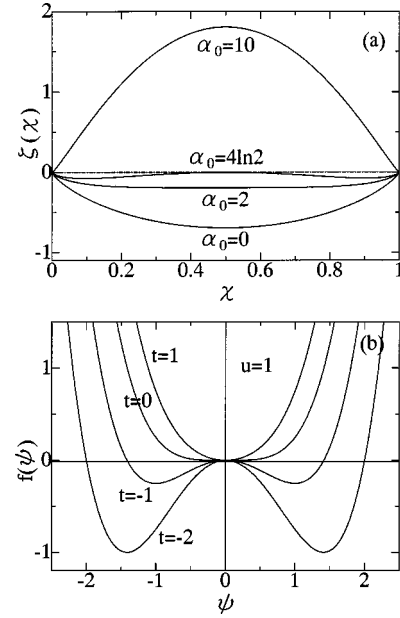


FIG. 1. (a) Behavior of $\zeta(\chi) = \chi \ln \chi + (1-\chi) \ln(1-\chi) + \alpha_0 \chi(1-\chi)$ with several values of the chiral discrimination coefficient α_0 . (b) Behavior of $f(\psi) = t\psi^2/2 + u\psi^4/4$ with several values of the coefficient t , and $u=1$.

crimination coefficient, with $w = (w_{LL} + w_{RR})/2 - w_{LR}$ denoting the difference of the nearest-neighbor interaction between identical and opposite enantiomers. λ_L is a Lagrange multiplier. It should be noted that k_2 is an odd function of $\chi - 1/2$. For simplicity, we take a first-order approximation that $k_2 = k_{20}(2\chi - 1)$, where k_{20} is the chiral modulus for pure left-handed materials. On the other hand, we assume that the tilt angle θ is a constant determined by the molecular area: $\cos \theta = V_0/A_0$, with V_0 being the molecular volume.

It is instructive to compare the free energy (2) with the SWBK energy (1). First, we readily find the homologous relations: $(\chi - 1/2) \leftrightarrow \psi$, and $k_{20} \leftrightarrow \lambda$. The mixing energy density $\zeta(\chi) = (k_B T/A_0)[\chi \ln \chi + (1-\chi) \ln(1-\chi) + \alpha_0 \chi(1-\chi)]$ is the counterpart of the Landau potential $f(\psi) = \frac{1}{2} t \psi^2 + \frac{1}{4} u \psi^4$. The pictures of both functions are plotted in Fig. 1, with similar behaviors of ramification. We show in Fig. 2 the bifurcation of χ_{\min} , at which the mixing energy is minimized, as a function of α_0 . As $\alpha_0 > 2$, the mixing energy density has two minima at χ_1 and $\chi_2 = 1 - \chi_1$.

Second, let us pay attention to the elastic energy. The projection of \mathbf{d} on the monolayer plane is often used as the 2D director $\hat{\mathbf{c}}$ (in the SWBK theory it is normalized). Substituting $\mathbf{d} = \hat{\mathbf{c}} \sin \theta + \hat{\mathbf{z}} \cos \theta$ and $\nabla = \nabla' + \hat{\mathbf{z}} \partial_z$ ($\nabla' = \hat{\mathbf{x}} \partial_x + \hat{\mathbf{y}} \partial_y$) into the elastic energy density in Eq. (2), we obtain its modified form in terms of $\hat{\mathbf{c}}$,

$$\frac{1}{2} K'_1 (\nabla' \cdot \hat{\mathbf{c}})^2 + \frac{1}{2} K'_3 (\nabla' \times \hat{\mathbf{c}})^2 + \lambda' (\chi - 1/2) (\nabla' \times \hat{\mathbf{c}}), \tag{3}$$

in which $K'_1 = k_{11} l \sin^2 \theta \cos \theta$, $K'_3 = (k_{22} \cos^2 \theta + k_{33} \sin^2 \theta) l \sin^2 \theta \cos \theta$, and $\lambda' = 2k_{20} l \sin \theta \cos^2 \theta$. This indicates the essential identity of the elastic energies in Eqs. (1) and (2).

Now we have to focus on the most critical difference between the SWBK theory and our approach. It is notable that the SWBK energy has a CSG term $(\nabla\psi)^2$. Usually, this

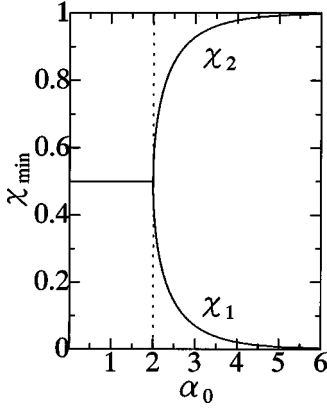


FIG. 2. χ_{\min} , the values of χ at minimum $\zeta(\chi)$ as a function of α_0 . As $\alpha_0=2$, there is a bifurcation of χ_{\min} . As α_0 further increases, the two values of χ_{\min} , denoted as χ_1 and χ_2 , quickly approach 0 or 1, respectively.

term is an essential part of a Ginzburg-Landau-type approach, and it is commonly believed that an expansion of the free energy of a molecular system in terms of concentration yields a CSG term and even higher-order gradient terms such as $(\nabla^2\psi)^2$ [25]. Evans gave a mathematical proof of the existence of these terms [26]. It should be emphasized that to obtain the free energy (2), we did not perform the Ginzburg-Landau expansion, but quoted the famous result about binary alloys by Bragg and Williams [24]. As mentioned earlier, Seul and Andelman reviewed two approaches to depict the spatial variation of concentration in Langmuir monolayers, one of which is to introduce a CSG term through the Ginzburg-Landau expansion, and the other is to consider a line tension at the boundaries instead. For the present topic, if we additionally introduce a CSG term $(\nabla\chi)^2$ into the free energy, there would be no essential difference between our approach and the SWBK theory, and consequently all the disagreements between the SWBK theory and the experimental results would occur similarly. With these considerations we shall proceed along with the second approach. We tentatively modify Eq. (2) by including a line energy,

$$\begin{aligned}
 F' = & \int \frac{1}{2}l \cos \theta [k_{11}(\nabla \cdot \mathbf{d})^2 + k_{22}(\mathbf{d} \cdot \nabla \times \mathbf{d})^2 \\
 & + k_{33}(\mathbf{d} \times \nabla \times \mathbf{d})^2 - 2k_2(\mathbf{d} \cdot \nabla \times \mathbf{d})] dA + \frac{k_B T}{A_0} \\
 & \times \int [\chi \ln \chi + (1-\chi) \ln(1-\chi) + \alpha_0 \chi(1-\chi)] dA \\
 & + \lambda_L \int (\chi - \frac{1}{2}) dA + \gamma L. \quad (4)
 \end{aligned}$$

As will be shown later, as CPS occurs, the chiral discrimination across domain boundaries naturally gives rise to a line tension. The line energy in Eq. (4) is fairly different from other terms in integral form. It reminds one of the line or wall defects in solids or bulk liquid crystals. Although each defect gives rise to an additional contribution to the total energy of the system, they are not treated directly in a continuum approach. For example, to obtain the director distribution in liquid crystals, one usually deals first with the elas-

tic energy and then discusses the consequent disclinations [23]. For the present topic, we follow this convention. First we deal with Eq. (2) to obtain possible patterns, then we discuss the effect of the line tension at the boundaries.

III. MATHEMATICS

Under the single-constant approximation ($k_{11}=k_{22}=k_{33}=k$) [23], a variational calculus on Eq. (2) leads the Euler-Lagrange equations to

$$\Delta \phi = \phi_{xx} + \phi_{yy} = \frac{2k_{20}}{k} \cot \theta [\chi_x \cos \phi + \chi_y \sin \phi], \quad (5)$$

$$\begin{aligned}
 \lambda_L + \frac{k_B T}{A_0} \left[\ln \frac{\chi}{1-\chi} + \alpha_0(1-2\chi) \right] \\
 - k_{20} l \cos \theta \sin 2\theta (\phi_x \cos \phi + \phi_y \sin \phi) = 0. \quad (6)
 \end{aligned}$$

To study the striped pattern, we take $\chi_y = \phi_y = 0$ and get the one-dimensional (1D) general solution

$$\cos \phi = \eta \frac{G'(\chi)}{\sqrt{G(\chi)}}, \quad (7)$$

$$\begin{aligned}
 x - x_0 = \frac{k \tan \theta}{8k_{20}} \\
 \times \int^x \frac{[G'(\chi')]^2 - 2G(\chi')G''(\chi')}{[G(\chi')]^{3/2} \{G(\chi') - \eta^2 [G''(\chi')]^2\}^{1/2}} d\chi'. \quad (8)
 \end{aligned}$$

Here $\eta = \sqrt{k_B T k} / (k_{20} \cos \theta \sqrt{8V_0})$ and $G(\chi) = C + \chi \ln \chi + (1-\chi) \ln(1-\chi) + \alpha_0 \chi(1-\chi)$, with C being an integral constant. $G'(\chi)$ and $G''(\chi)$ are the first and second derivatives, respectively.

To understand the meaning of this solution, we at first take a second-order approximation $G(\chi) \approx C - \ln 2 + \alpha_0/4 + (2-\alpha_0)(\chi-1/2)^2$. It leads Eqs. (7) and (8) to the solution in Ref. [22]. Noting that the fourth-order term, which is necessary to keep the system thermodynamically stable if $\alpha_0 > 2$, is neglected, we can recognize that the second-order solution is at most a ‘‘weak’’ CPS.

As shown in Fig. 1(a), as $\alpha_0 > 2$, the mixing energy has two minima at $\chi = \chi_1$ and χ_2 . The energy difference between the racemic mixture ($\chi \equiv 1/2$) and the CPS state ($\chi = \chi_1$ or χ_2) increases quickly with α_0 . This implies that as $\alpha_0 \gg 2$, if all CPS domains have chiral order parameters $\chi = \chi_1$ or χ_2 , the mixing energy as well as the total energy would be greatly decreased. This prompts us to seek a solution to Eqs. (5) and (6) consisting of several domains with alternate chiralities χ_1 and χ_2 . In fact we found that this solution, in the 1D case, is nothing but the extremity of Eqs. (7) and (8) with the integral constant $C = -(\chi_1 \ln \chi_1 + \chi_2 \ln \chi_2 + \alpha_0 \chi_1 \chi_2)$. As C equals this special value, Eqs. (7) and (8) are simplified to a series of stripes $\dots L_1, L_2, L_3, L_4 \dots$ schematically shown in Fig. 3, with alternate chiralities

$$\phi \equiv \pi/2, \quad \chi = \begin{cases} \chi_1, & x \in \dots L_1, L_3, \dots \\ \chi_2, & x \in \dots L_2, L_4, \dots \end{cases} \quad (9)$$

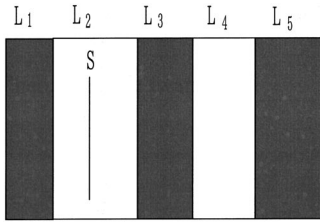


FIG. 3. Schematic of striped pattern.

It is noticeable that this solution predicts a uniform azimuthal angle ϕ within each stripe. This is distinct from the striped patterns obtained by SWBK, in which the azimuth ϕ varies sinusoidally or linearly with position. This offers a possible explanation for the homogeneous molecular orientation within each domain observed on the Langmuir and LB films. The abrupt chirality changes at the boundaries between adjacent domains is also in accordance with the experimental results, as discussed earlier.

IV. DISCUSSION

The existence of solution (9) is a reflection of the difference between the two approaches discussed previously [18]. In fact, in the Ginzburg-Landau theory the abrupt change of chirality χ is forbidden. In the present study, the chiral discrimination naturally yields a line tension at boundaries. As shown in Fig. 3, the molecular interaction across an edge is different from that across a line in a homogeneous domain (such as line S in stripe L_2). The line tension at boundaries, γ , is by definition the difference per unit length between these two interactions. Considering only the nearest-neighbor interaction, it can be roughly estimated that

$$\gamma = 2\rho(\chi_2 - \chi_1)^2 w. \quad (10)$$

Here ρ is the molecular line density along the boundaries. As CPS occurs, it always stands that $\gamma > 0$, since $\chi_1 \neq 1/2$. In the strong CPS case in which $\chi_1 \approx 0$ and $\chi_2 \approx 1$, we have $\gamma \approx 2\rho w$, which is just the chiral discrimination per unit length between two pure enantiomeric phases. We refer the line energy associated with Eq. (10) to the last term in Eq. (4).

It is a little puzzling that the present model cannot predict the stripe width of pattern (9), since Eq. (8) is singular as $C = -(\chi_1 \ln \chi_1 + \chi_2 \ln \chi_2 + \alpha_0 \chi_1 \chi_2)$. On the other hand, the presence of the line tension indicates that the longer the total edge, the higher the whole energy. This leads to a natural conclusion that the energy-minimized pattern is a two-domain one in which all molecules segregate into a left-handed domain with $\chi = \chi_1$ and a right-handed one with $\chi = \chi_2$ [this is a special case of Eq. (9)]. However, it does not indicate that other patterns depicted by Eq. (9) are forbidden. In fact, it is possible that a metastable multistripe pattern could occur; i.e., once a multistripe pattern comes into being in the CPS process, it would be difficult for it to evolve into a two-domain pattern if each stripe were wide enough, since usually the 2D diffusion is rather slow. In other words, although the two-domain pattern is energetically advantageous, it is quite difficult to reach in a large-area monolayer, and instead a multistripe pattern may be easier to observe. What kind of pattern occurs should be determined by the

process of CPS, which is fairly stochastic. As a consequence, the widths of stripes are diversified, which is consistent with the experimental results.

Although a detailed discussion about the stochastic process of pattern formation does not belong to the present work, which is a mean-field approach, a simple exploration is beneficial for understanding the physical picture. The key point is that the chiral discrimination coefficient α_0 is a function of the molecular area A_0 (similar to the Landau theory in which the coefficient of the second-order term is associated with temperature), and in compression-induced CPS α_0 should grow with decreasing A_0 . The compression-induced CPS is depicted qualitatively as follows. As molecular area A_0 is quite large, α_0 is small and the monolayer is racemic. When the compression raises α_0 to the threshold 2 (Fig. 2), microscopically, the two kinds of enantiomers begin to collect, respectively. Further compression enhances α_0 successively and at last leads to a strong CPS (in the experiment by Eckhardt *et al.* α_0 can be as large as 14.2 under compression, as pointed out in [22]). In this process, small domains may appear at the beginning of CPS, since the two enantiomers have to collect at a small scale, respectively. However, owing to the line tension, domains with identical chiralities would rather converge with each other, until the distance between any two domains with identical chiralities is too wide for molecules to cross over. At last the monolayer reaches a metastable state consisting of parallel stripes with diversified widths. We refer the AFM image shown in Ref. [12] to this metastable pattern.

V. CONCLUSIONS

In this paper, we have analyzed the compression-induced CPS in Langmuir monolayers. The CPS boundaries are viewed as walls with finite line tension originated from chiral discrimination. Our model predicts uniform stripes, diversity of stripe widths, and abrupt changes of chiral order parameter at boundaries. Qualitatively, this picture is in accordance with the existing observations. Future experimental examination should be based on these predictions, especially the uniformity of stripes and the diversity of stripe widths and domain sizes.

There is another aspect that may be more significant than the topic of CPS itself. As indicated by Seul and Andelman [18], in the analysis of the phase separation of a mixture, the CSG term is equivalent in a sense to a line tension at phase boundaries. This may be a favorite point of view at present. The comparison of the present work with the SWBK theory shows that these two approaches lead to very different consequences in the particular contexts. Considering the importance of the CSG term in the analysis of multiphase phenomena and the extensive applications of both approaches, it may be of essential significance to clarify such questions as in which case the CSG term and the line tension are equivalent and in which case are they not, and in which case it is better to apply the CSG term and in which case should a line tension be employed. These questions are far beyond the scope of the present work.

APPENDIX

A valuable analysis about how a CSG term equivalently yields a surface tension between two phases of a binary alloy

has been given by Cahn and Hilliard [21]. Here we give a parallel manifestation for the CPS of a racemic film. The free energy of the film is written as

$$F = L \int \left[\frac{1}{2} \kappa \left(\frac{d\psi}{dx} \right)^2 + f_0(\psi) \right] dx, \quad (\text{A1})$$

where $f_0(\psi)$, the free energy per unit area of a mixture of uniform composition ψ , is a W -form function of ψ with two minima at $\psi = \pm \psi_m$.

The line tension is expressed as

$$\gamma = \int_{-\infty}^{+\infty} \left[\frac{1}{2} \kappa \left(\frac{d\psi}{dx} \right)^2 + \Delta f(\psi) \right] dx, \quad (\text{A2})$$

where $\Delta f(\psi) = f_0(\psi) - f_0(\psi_m)$. With the boundary conditions $\psi \rightarrow \pm \psi_m$ as $x \rightarrow \pm \infty$, we get the Euler-Lagrange equation through variational calculus

$$\frac{1}{2} \kappa \left(\frac{d\psi}{dx} \right)^2 = \Delta f(\psi), \quad (\text{A3})$$

and minimize Eq. (A2) to

$$\gamma = \int_{-\psi_m}^{\psi_m} \sqrt{2\kappa \Delta f(\psi)} d\psi. \quad (\text{A4})$$

SWBK assumed that $f_0(\psi) = \frac{1}{2}t\psi^2 + \frac{1}{4}u\psi^4$. Substituting it into Eq. (A4) we get

$$\gamma = \frac{2|t|}{3u} \sqrt{2\kappa|t|}. \quad (\text{A5})$$

Summarily, in this sense a CSG term is equivalent to a line tension. But this is by no means to say that the two approaches always have identical performances. In particular contexts it is possible that one approach is more realistic and more fruitful than the other.

-
- [1] L. Pasteur, C. R. Hebd. Seances Acad. Sci. **26**, 535 (1848).
 [2] A. Collet, M.-J. Brienne, and J. Jacques, Chem. Rev. **80**, 215 (1980).
 [3] J. Jacques, A. Collet, and S. H. Wilen, *Enantiomers, Racemates and Resolutions* (Wiley, New York, 1981).
 [4] D. Andelman and P. G. de Gennes, C. R. Acad. Sci. (Paris) **307**, 233 (1988); D. Andelman, J. Am. Chem. Soc. **111**, 6536 (1989).
 [5] P. Nassoy, M. Goldmann, O. Bouloussa, and F. Rondelez, Phys. Rev. Lett. **75**, 457 (1995).
 [6] M. V. Stewart and E. M. Arnert, in *Topics in Stereochemistry*, edited by N. L. Allinger, E. L. Eliel, and S. H. Wilen (Wiley, New York, 1982).
 [7] J. MacLennan and M. Seul, Phys. Rev. Lett. **69**, 2082 (1992); **69**, 3267 (1992); J. E. MacLennan, U. Sohling, N. A. Clark, and M. Seul, Phys. Rev. E **49**, 3207 (1994).
 [8] J. Pang and N. A. Clark, Phys. Rev. Lett. **73**, 2332 (1994).
 [9] D. K. Schwartz, Nature (London) **362**, 593 (1993).
 [10] X. Qiu, J. Ruiz-Garcia, K. J. Stine, C. M. Knobler, and J. V. Selinger, Phys. Rev. Lett. **67**, 703 (1991).
 [11] X. Qiu, J. Ruiz-Garcia, and C. M. Knobler, in *Interface Dynamics and Growth*, edited by K. S. Liang, M. P. Anderson, R. F. Bruinsma, and G. Scoles, MRS Symposia Proceedings No. 23 (Materials Research Society, Pittsburgh, 1992), p. 263.
 [12] C. J. Eckhardt, N. M. Peachey, D. R. Swanson, J. M. Takacs, M. A. Khan, X. Gong, J.-H. Kim, J. Wang, and R. A. Uphaus, Nature (London) **362**, 614 (1993).
 [13] F. Charra and J. Cousty, Phys. Rev. Lett. **80**, 1682 (1998).
 [14] R. Viswanathan, J. A. Zasadzinski, and D. K. Schwartz, Nature (London) **368**, 440 (1994).
 [15] J. V. Selinger, Z.-G. Wang, R. F. Bruinsma, and C. M. Knobler, Phys. Rev. Lett. **70**, 1139 (1993).
 [16] J. V. Selinger and R. L. B. Selinger, Phys. Rev. E **51**, R860 (1995).
 [17] T. Ohyama, A. E. Jacobs, and D. Mukamel, Phys. Rev. E **53**, 2595 (1996).
 [18] M. Seul and D. Andelman, Science **267**, 476 (1995).
 [19] D. Andelman, F. Brochard, and J.-F. Joanny, J. Chem. Phys. **86**, 3673 (1987).
 [20] D. Andelman, F. Brochard, P. G. de Gennes, and J.-F. Joanny, C. R. Acad. Sci. (Paris) **301**, 675 (1985); D. J. Keller, J. M. McConnell, and V. T. Moy, J. Phys. Chem. **90**, 2311 (1986); A. Fischer, M. Lösche, H. Möhwald, and E. Sackmann, J. Phys. (France) Lett. **45**, L785 (1984).
 [21] J. W. Cahn and J. E. Hilliard, J. Chem. Phys. **28**, 258 (1958).
 [22] M. Iwamoto, C.-X. Wu, and Z.-C. Ou-Yang, Phys. Rev. E **59**, 586 (1999).
 [23] P. G. de Gennes and J. Prost, *The Physics of Liquid Crystals*, 2nd ed. (Clarendon, Oxford, 1993).
 [24] W. L. Bragg and E. J. Williams, Proc. R. Soc. London, Ser. A **145**, 699 (1934).
 [25] G. Gompper and M. Schick, *Self-Assembling Amphiphilic Systems* (Academic, New York, 1994).
 [26] R. Evans, Adv. Phys. **28**, 143 (1979).